Deblending Using Focal Transformation with a Greedy Inversion Solver

Cao, J.; Kontakis, Apostolos; Verschuur, Eric; Gu, H.

DOI
10.3997/2214-4609.201701372

Publication date
2017

Document Version
Final published version

Published in
Proceedings of 79th EAGE Conference and Exhibition 2017

We P3 14

Deblending Using Focal Transformation with a Greedy Inversion Solver

J. Cao* (China University of Geosciences (Wuhan)), A. Kontakis (Delft University of Technology), D.J. Verschuur (Delft University of Technology), H. Gu (China University of Geosciences (Wuhan))

Summary

In this work, we adopt a greedy inversion solver to design a fast version of the double focal transform that we can use to eliminate blending noise in simultaneous source acquisition. The greedy inversion introduces a coherence-oriented mechanism to enhance focusing of significant model space, leading to a sparse model space and fast convergence rate. Synthetics and numerically blended field data examples demonstrate the validity of its application for deblending. We also tested different inversion

parameters (percentile value and weights) influencing the choice of the model subspace. The results indicate that by setting the percentile carefully and using weights it is possible to get better deblending results.

Introduction

Several simultaneous source data acquisition methods have been proposed to reduce the cost of seismic surveys, which also offer certain advantages over conventional acquisitions such as better illumination of the subsurface and better spatial resolution (Berkhout, 2008). One way to handle the blended data is to use it for imaging directly (Soni and Verschuur, 2015). However, most seismic data processing algorithms are designed to handle data with nonoverlapping sources. This makes it necessary to separate the blended shot gathers first (deblending) and then to process them in the conventional way. Deblending methods can be sorted into three categories: (1) Denoising–based source separation (Huo et al., 2012a); (2) Source coding-based source separation (Muller et al., 2015); (3) Inversion-based source separation (Moore et al., 2010), usually with constraints designed to take advantage of signal coherency.

Central to the deblending approach described in this paper is the focal transform. The first variant was proposed by Berkhout and Verschuur (2006), which uses subsurface information from the data to create two-way focal operators. A second variant was proposed in Berkhout and Verschuur (2010), using one-way propagation operators. Kontakis and Verschuur (2014) use the sparse double focal transform for solving the deblending problem and get an inspiring simultaneous source separation result. In this paper, we propose a new method for deblending that uses the double focal transform in combination with a greedy solver for faster convergence. We then examine its performance on synthetic and numerically-blended field data.

Theory

The double focal transform is a versatile seismic processing tool that uses one-way extrapolation operators to generate wavefields focused at chosen depth levels. Combined with sparsity-based inversion, it is possible to transform the surface data into a compressed focal domain with few elements of significant magnitude. This sparse representation of the recorded wavefield is an attractive property of the focal transform, that can be exploited for solving inherently under-determined problems, such as interpolation and deblending. An example of such a sparse inversion is the optimization problem

$$\min_{\delta\mathbf{X}_1,\ldots,\delta\mathbf{X}_K} \left\{ \sum_t \sum_{k=1}^{K} \left\| \delta \mathrm{X}_k \right\|_S \right\} \text{ s.t. } \sum_w \left\| \mathrm{P} - \sum_{k=1}^{K} \mathrm{W}_k^- \delta \mathrm{X}_k \mathrm{W}_k^+ \right\|_F \le \sigma \quad . \tag{1}$$

Here K pairs of focal operators W_k^- and W_k^- are used. Each pair of focal operators defines a focal subdomain, $\delta \mathrm{X}_k$, that holds the focal representation of the input surface data, P. The notation $\|.\|_S$ and $\|.\|_F$ is used for the sum and Frobenius norm respectively. All operators are in the temporal frequency domain, except when marked with a hat symbol, in which case they are in the time domain. Adding a blending operator $\mathbf{\Gamma}$ to Equation (1) yields

$$\min_{\delta\mathbf{X}_1,\ldots,\delta\mathbf{X}_K} \left\{ \sum_t \sum_{k=1}^{K} \left\| \delta \mathrm{X}_k \right\|_S \right\} \text{ s.t. } \sum_w \left\| \mathrm{P}_{\mathrm{bl}} - \sum_{k=1}^{K} \mathrm{W}_k^- \delta \mathrm{X}_k \mathrm{W}_k^+ \Gamma \right\|_F \le \sigma \quad , \tag{2}$$

which can be used for deblending (Kontakis and Verschuur, 2014). Note that in (2) the blended data P_{bl} is given as an input. Optimization problems of the form (1) and (2) can be handled by solvers such as SPGL1 solver (van den Berg and Friedlander, 2008).

In this paper we do not perform deblending by solving the optimization problem (2). Instead, inspired by the greedy local Radon transform (Wang et al., 2010), we use a greedy least-squares method for the same purpose. The alternative deblending procedure we use can be described as follows:

1. Set the maximum number of iterations M and the percentile θ to desired values. The percentile θ controls the sparsity of the focal subdomains.

2. Set the data residual $\mathrm{P}_{\mathrm{bl,res}}^{[0]} = \mathrm{P}_{\mathrm{bl}}$, the deblended focal subdomains $\delta\mathrm{X}_{k,\mathrm{debl}}^{[0]} = 0$ and the iteration counter $i = 0$.
3. While $i < M$
   (a) Pseudodeblend the residual, $\mathrm{P}_{\mathrm{ps,res}}^{[i]} = \mathrm{P}_{\mathrm{bl,res}}^{[i]}\Gamma^{H}$, where Γ^{H} is the adjoint of the blending operator.
   (b) Focus the pseudodeblended residual at each depth level and place the results into an array
   $$\left(\delta\mathrm{F}_1^{[i]},...,\delta\mathrm{F}_K^{[i]}\right) = (\mathrm{W}_1^{-H}\mathrm{P}_{\mathrm{ps,res}}^{[i]}\mathrm{W}_1^{+H},...,\mathrm{W}_K^{-H}\mathrm{P}_{\mathrm{ps,res}}^{[i]}\mathrm{W}_K^{+H}) \ .$$
   Note that each $\delta\mathrm{F}_k^{[i]}$ has focused, but not yet sparse data.
   (c) Vectorise the array $\left(\delta\mathrm{F}_1^{[i]},...,\delta\mathrm{F}_K^{[i]}\right)$ and select the top 1 - θ percent of the elements with the highest magnitudes. The indices of those elements define a model subspace $\chi^{[i]}$.
   (d) Solve the constrained least-squares problem (e.g. using LSQR)
   $$\left(\Delta\mathrm{X}_{1,\mathrm{debl}}^{[i]},...,\Delta\mathrm{X}_{K,\mathrm{debl}}^{[i]}\right) = \underset{\substack{\delta\mathrm{X}_k \in \chi^{[i]} \\ k=1,2,...,K}}{\arg\min}\left\{\sum_w \left\| \mathrm{P}_{\mathrm{bl,res}}^{[i]} - \sum_{k=1}^{K}\mathrm{W}_k^{-}\delta\mathrm{X}_k\mathrm{W}_k^{+}\Gamma \right\|_F\right\}.$$
4. Update the model parameters
   $$\delta\mathrm{X}_{k,\mathrm{debl}}^{[i+1]} = \delta\mathrm{X}_{k,\mathrm{debl}}^{[i]} + \Delta\mathrm{X}_{k,\mathrm{debl}}^{[i]}, \ k = 1,2,...,K \ .$$
5. Update the deblended data estimate, the blended data residual
   $$\mathrm{P}_{\mathrm{debl}}^{[i+1]} = \sum_{k=1}^{K}\mathrm{W}_k^{-}\delta\mathrm{X}_{k,\mathrm{debl}}^{[i+1]}\mathrm{W}_k^{+}, \ \mathrm{P}_{\mathrm{bl,res}}^{[i+1]} = \mathrm{P}_{\mathrm{bl}} - \mathrm{P}_{\mathrm{debl}}^{[i+1]}\Gamma \ .$$
6. Increase the iteration counter.

The final deblended data is then given by $\mathrm{P}_{\mathrm{debl}} = \mathrm{P}_{\mathrm{debl}}^{[M-1]}$. The constraint that the solution should lie in a restricted subspace of the focal subdomains favors sparse solutions and suppresses blending noise. Apart from a percentile-based approach, it is possible to use thresholding techniques to select the model subspace. There is a trade-off between choosing a percentile that is conservative enough to prevent blending noise entering the solution, and one generous enough such that the process converges in the fewer number of iterations necessary.

Example 1: Synthetic data

We first evaluate the proposed method on a set of simple synthetics, composed of 3 reflection events with hyperbolic moveout (Figure 1a). The deblending quality is evaluated using the following expression

$$Q = 10\log_{10}\left(\frac{\sum_w \|\mathrm{P}\|_F^2}{\sum_w \|\mathrm{P} - \mathrm{P}_{\mathrm{debl}}\|_F^2}\right) \quad . \tag{3}$$

With $\theta = 99.8\%$ and using radial weights mask on the focal subdomains before choosing the subspace $\chi^{[i]}$, we get a high Q value for the deblending result after 20 iterations, as shown in Figure 1c. The difference between the unblended and the deblended data in the errors profile (Figure 1d) is minimal, demonstrating good separation (here Q=36.46 dB).

We test the same parameters as Figure 1, except without using radial weights to show the importance of using such weights. Looking at Figure 2c it can be seen that when not using weights, much more blending noise has been included in the solution compared to the result using weights (Figure 2b). This happens because the blending noise may be still strong despite the fact that it does not focus as point out by the arrow in Figure 2a. Using weights during the subspace selection can help avoid the cases described above. Looking at Figure 2d, using $\theta = 99.6\%$ and radial weights, more blending

noise is visible and, thus, we should set the percentile carefully to get optimum deblending results.

Example 2: Numerically blended field data

The performance of the greedy approach is also tested using a North Sea dataset. We choose a subset of 151 sources and 151 receivers. The extracted data is then numerically blended with a blending factor of 2. The first unblended and blended shot gathers are shown in Figure 3a and 3b. After deblending using the greedy method, we get good results with a Q value of 13.65 dB, after 40 iterations, although some blending noise is still present in the deblending result, as shown in Figure 3d.

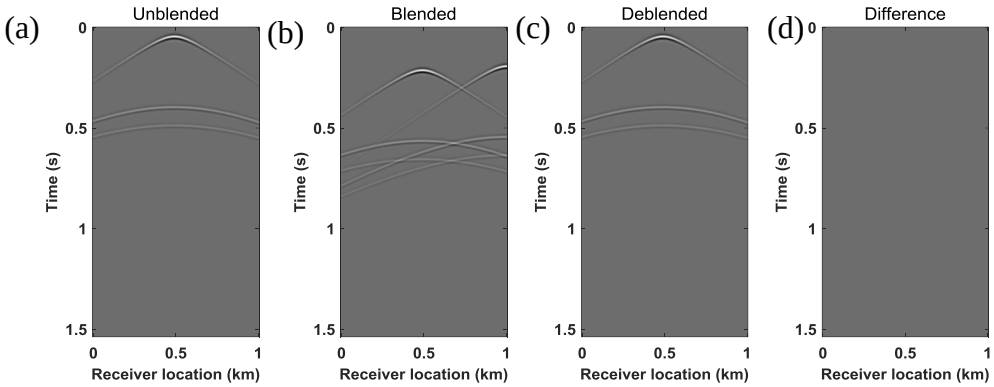

Figure 1 *(a) Original unblended shot gather, (b) blended shot gather, (c) deblended shot gather after 20 iterations of greedy focal transform with* $\theta = 99.8\%$ *and using radial weights, (d) the difference between the Figure 1a and Figure 1c.*

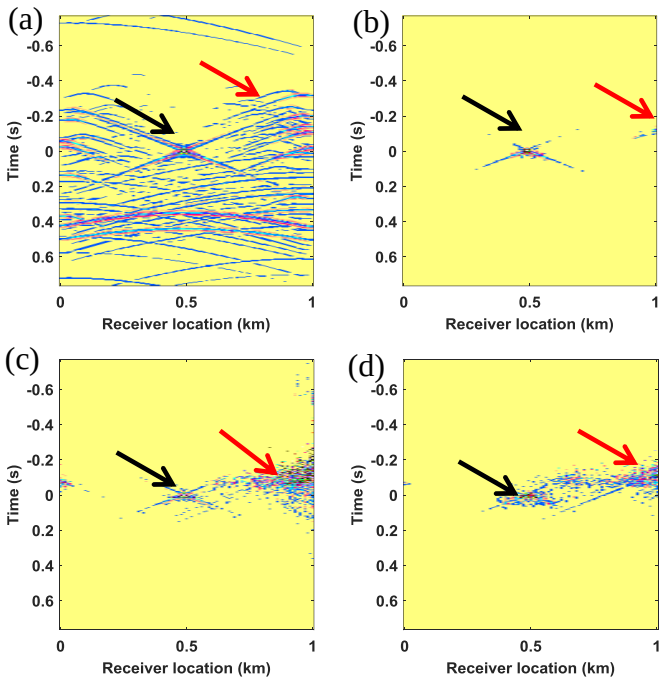

Figure 2 *Focused shot gather, (a) before deblending, (b) after 20 iterations of deblending using* $\theta = 99.8\%$ *and radial weights, (c) after 20 iterations of deblending with* $\theta = 99.8\%$ *and no weights, (d) after 20 iterations of deblending using* $\theta = 99.6\%$ *and radial weights. Red arrows point to the blending noise and black arrows to signal.*

Conclusions

We have implemented a fast, greedy version of the double focal transform. Synthetics and numerically blended field data examples demonstrate the validity of its application for deblending. We also tested different inversion parameters (percentile value and weights) influencing the choice of the model subspace. The results indicate that by setting the percentile carefully and using weights it is possible to get better deblending results. Although in this paper, we only show the application of this new method for deblending, it is straightforward to modify it for the purpose of data reconstruction using the focal transform or to combine it with other transforms.

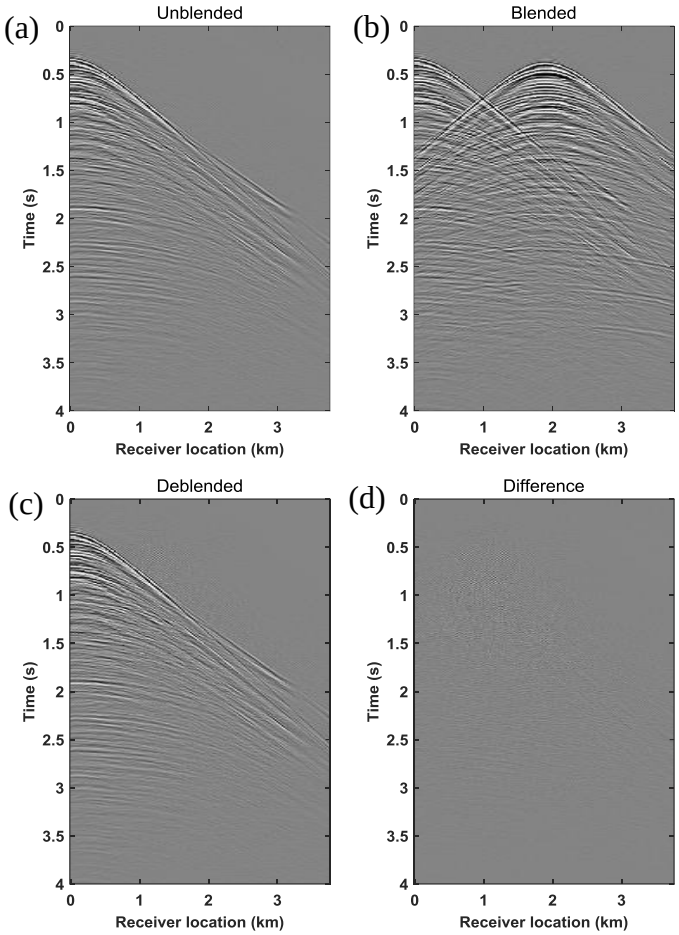

Figure 3 *(a) Original unblended shot gather, (b) blended shot gather, (c) deblended shot gather after 40 iterations of greedy focal deblending with* $\theta = 99.8\%$ *and using weights, (d) the difference between the Figure 3a and Figure 3c.*

Acknowledgements

The authors would like to thank Statoil for providing the North Sea field data. This work is also funded by China Important National Sciences & Technology Specific Projects (2016ZX05024-005-002).

References

Berkhout, A. J. [2008] Changing the mindset in seismic data acquisition. *The Leading Edge*, **27**(7), 924–938.

Berkhout, A. J. and Verschuur, D. J. [2006] Focal transformation, an imaging concept for signal restoration and noise removal. *Geophysics*, **71**(6), A55–A59.

Berkhout, A. J. and Verschuur, D. J. [2010] Parameterization of seismic data using gridpoint responses. *80th SEG Annual International Meeting*, Expanded Abstracts, 3344–3348.

Huo, S., Luo, Y. and Kelamis, P. G. [2012a] Simultaneous sources separation via multidirectional vector-median filtering. *Geophysics*, **77**(4), V123–V131.

Kontakis A. and Verschuur, D. J. [2014] Deblending via sparsity-constrained inversion in the focal domain. *76th EAGE Conference and Exhibition*, Expanded Abstracts, Th ELI2 02.

Mueller, M.B., Halliday, D. F., van Manen, D. J., and Robertsson, J. O. A. [2015] The benefit of encoded source sequences for simultaneous source separation. *Geophysics*, **80**(5), V133-V143.

Soni, A. K. and Verschuur, D. J. [2015] Imaging blended vertical seismic profiling data using full-wavefield migration in the common-receiver domain. *Geophysics*, **80**(3), R123-R138.

van den Berg, E. and Friedlander, M. P. [2008] Probing the pareto frontier for basis pursuit solutions. *SIAM Journal on Scientific Computing*, **31**(2), 890-912.

Wang J., Ng, M. and Perz, M. [2010] Seismic data interpolation by greedy local Radon. *Geophysics*, **75**(6), WB225–WB234.